Improved Field Evaluation of Reference Cell Using Spectral Measurements

Frank Vignola[1], Josh Peterson[1], Richard Kessler[1], Vikram Sandhu[1], Aron Habte[2], Manajit Sengupta[2]

[1]University of Oregon, Eugene, Oregon, 97403, USA,
[2]National Renewable Energy Laboratory, Golden, Colorado, 80301, USA

***Abstract* —Output from a reference solar cell mounted on a one-axis tracking surface is investigated using 350 nm to 1650 nm spectral irradiance measurements on selected days throughout the year. Comparisons are made to a Class-A pyranometer also mounted on the tracking surface. The ratio of the reference cell's measurements to reference pyranometer measurements exhibit systematic biases over the day and year. Most of this bias is linked to spectral, temperature, and angle-of-incident effects that differ for the reference cell and the pyranometer. The comparison is done for selected clear and totally cloudy days to determine the magnitude of the effects and to characterize they influence the measurements made with reference cells.**

***Index Terms* —Reference solar cells, spectral measurements, one-axis tracker, pyranometer, resource assessment**

I. Introduction

Reference solar cells are constructed similar to solar modules with the same solar cells, glazing, encapsulant, and backing as photovoltaic (PV) modules except they are operated at short circuit current and hence do not need an inverter or max power point tracker to operate. Reference cells are often used to validate module flash tests during production to ensure that the modules meet specifications.

Reference cells are also used in the field to evaluate the performance of PV systems. Reference cells placed in the plane of array of the PV system are useful in that they have the same spectral and cosine response of the PV modules they are testing. Pyranometers in the plane of array are designed to measure incident radiation that are used as inputs into software programs that estimate PV system performance.

The advantage of reference cells is that they incorporate spectral dependence and plane of array effects that do not have to be modeled. Since modeling introduces uncertainties, performance estimates using reference cells should result in smaller uncertainties. The disadvantage associated with reference cells is that they are not pyranometers and measurements at one angle and orientation cannot be easily translated to values at different tilts and orientations. As with pyranometers, the effect of temperature on reference cell measurements and transference from short circuit current to max power point values require modeling.

Reference cells differ from PV modules in that their output is measured in a short circuit current configuration. Short circuit current is proportional to incident radiation and typically the short circuit current increases slightly with temperature increase. However, reference cells are not pyranometers and when reference cells are compared to pyranometer measurements large biases are apparent. Three main sources of these biases are the spectral response of the reference cell, the deviation from an ideal cosine response, and a temperature effect [1]-[3]. When evaluating these comparisons, it is important to also consider the systematic biases associated with the comparison pyranometer as well as the reference cell.

Understanding the characteristics and biases of reference cells are not only essential for proper evaluation of the PV arrays, they are also important when one is contrasting reference cell measurements at different tilts and orientations, comparing results with various pyranometer measurements, and studying PV system performance using the reference cells.

This study differs from previous studies because spectral measurements, not modeled spectral distributions, are used to calculate the effect of changing spectral distributions over the day on the reference cell measurements. By using spectral measurements, some of the uncertainties associated with the modeled spectral distribution are eliminated.

The experimental data used for this study comes from co-located spectral and reference cell instruments on a one-axis tracker located at the National Renewable Energy Laboratory's (NREL) Solar Radiation Research Laboratory (SRRL) in Golden, Colorado. Measurements made on a one-axis tracking surface minimizes, but does not eliminate the angle-of-incidence (AOI) effects. The present study finds that accounting for differences in the spectral distribution can only partially be addressed by spectral measurements in the 350 to 1650 nm range even though the reference cell does not respond to wavelength greater than 1250 nm. The spectral characteristics of the temperature effects on reference cell output are also taken into account. Overall there is good agreement between the broadband pyranometer readings and reference cell measurements after adjustments have been made for spectral, temperature, AOI effects. However, some differences remain and these differences will be discussed.

This article is organized as follows. First the experimental equipment and arrangement are described along with the uncertainty in the data. The ratio of the reference solar cell output to the reference Class-A pyranometer is used to compare the results over a variety of days under different weather conditions. An analysis under clear sky conditions is then conducted. Modeled effects for temperature and spectral radiation are then performed. Measured spectral data are used

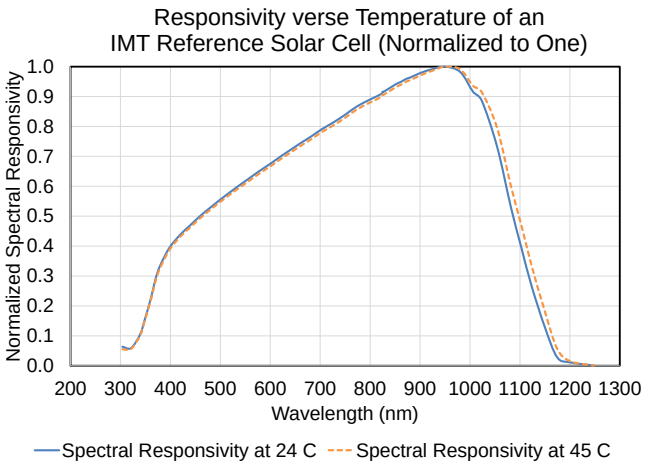

Fig. 1. Spectral responsivity of a reference cell normalized to one at 950 nm. Measurements made at 24ºC and 45ºC under a NIST calibrated lamp.

in this analysis. The measured and modeled ratios are then compared and differences are examined. The magnitude and nature of these differences are described. A summary of the findings is then presented along with suggestions on how to improve the analysis.

II. Experimental Setup

Data for this study comes from reference cells, pyranometers, and spectroradiometers co-located on a one-axis EKO tracker in Golden, Colorado. Comparisons are made between high quality pyranometer measurements (using a Kipp & Zonen CMP 22) and IMT reference cells on a one-axis tracker. Every five minutes, the EKO WISER spectroradiometers generated spectral data from 350 to 1650 nm with calibration traceability to a NIST lamp. This calibration was performed with the spectroradiometer perpendicular to the light source. No dependence on cosine response was measured at the time of calibration. The IMT reference cell was calibrated at NREL against a standard lamp and its spectral dependence was determined. Again, the reference cell response was measured perpendicular to the light source. This spectral responsivity was measured at three temperatures (24, 35, 45 ºC). The temperature of the reference cell is measured along with its voltage output. The CMP 22 is a Class-A pyranometer and was calibrated using the NREL BORCAL protocol. The uncertainty in the pyranometer's minute values is approximately ±3.5% at a 95% level of confidence for irradiance measurements greater than 100 W/m^2.

The EKO one-axis tracker is aligned north-south and the platform faces east at sunrise. At solar noon, the solar zenith angle is at minimum, the platform is horizontal. The range of motion of the tracker as used in this experiment only allowed the zenith angle of the tracker to rotate from 90° - 0º (as opposed to 90° – -90º). In order to get the afternoon data, at solar noon the tracker rotates the azimuthal orientation of the platform by 180º. The tracker then rotates the platform until it faces west at sunset. With adaptations, it is also possible to have a continuous rotation from east to west, but this isn't how the tracker was configured for the data used in this experiment.

The spectral responsivity of the reference cell is shown in Fig. 1. The responsivity peaks around 950 nm and is zero above 1250 nm. The spectral responsivity at wavelengths above 950 nm increase as temperature increase.

The increase in spectral responsivity at higher temperatures for wavelengths greater than 1000 nm is caused by the kinetic energy increase of the electrons. The energy of the photon not only has to be sufficient to separate the electron from the atom, it has to impart enough energy so that the electron can jump across the band gap. Under short circuit configuration, as the temperature increases, the kinetic energy of the electrons increase. For electrons with energies just below the level necessary to jump into the conduction band, the additional kinetic energy adds just enough addition energy to some electrons so that they can jump across the band gap. This kinetic energy boost mainly affects electrons separated from atoms by photons with longer wavelengths, in the 1000 nm to 1250 nm range, enabling a few more electrons to jump the gap. A more thorough discussion of this effect can be found in [4].

III. Calculation of Average IMT Responsivity

With the spectral data from the spectroradiometer it is possible to determine the average responsivity of the IMT reference cell (see Eqn. 1). On clear days, the distribution of incident radiation changes throughout the day as path length through the atmosphere changes. The changing spectral distribution will change the average responsivity of the IMT.

In Fig. 2, the relative intensity of spectral irradiance verses wavelength is shown at various times for a day without clouds. To compare the relative intensity of the spectral radiation at each wavelength, the spectral intensity is divided by the intensity of the spectral radiation at 500 nm. There is a significant shift in spectral distribution in the early morning (6:00 – SZA=87º) and late evening hours (17:30 – SZA=82.5º). Once the sun reaches a zenith angle below 65º the spectral distribution has minimal changes assuming the aerosol and water vapor content of the atmosphere has minimal change.

The average responsivity of the IMT reference cell is given by Eqn. 1. The spectral responsivity of the reference cell, adjusted for temperature, is multiplied the spectral irradiance of the incident solar radiation. This product is summed over all wavelengths and divided by the sum of the spectral irradiance over all wavelengths.

$$\overline{R} = \frac{\sum_{280\ nm}^{4000\ nm} R_\lambda \cdot [1 + T_\lambda \cdot (T_{amb} - 25)] \cdot I_\lambda}{\sum_{280\ nm}^{4000\ nm} I_\lambda} \qquad \text{Eqn. 1}$$

where R_λ is the IMT responsivity at wavelength λ and I_λ is the intensity of the radiation at wavelength λ, T_λ is the effect of

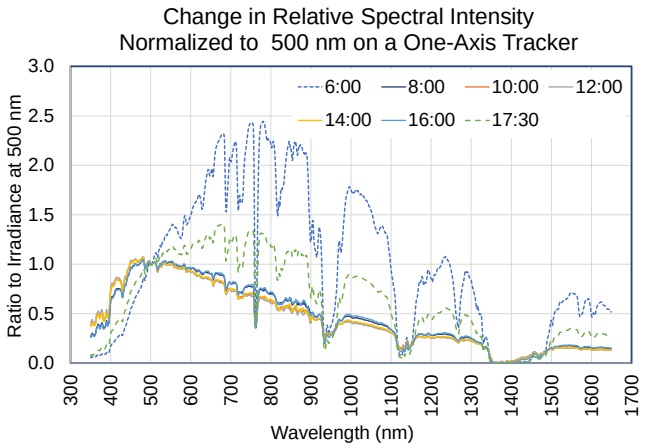

Fig. 2. Relative change in clear sky spectral intensity at different times of day normalized to one at 500 nm on September 13, 2018. Early morning (6:00 – SZA = 87°) and late afternoon (17:30 – SZA = 82.5°) exhibit a dramatic shift in the spectral distribution from distributions during the middle of the day.

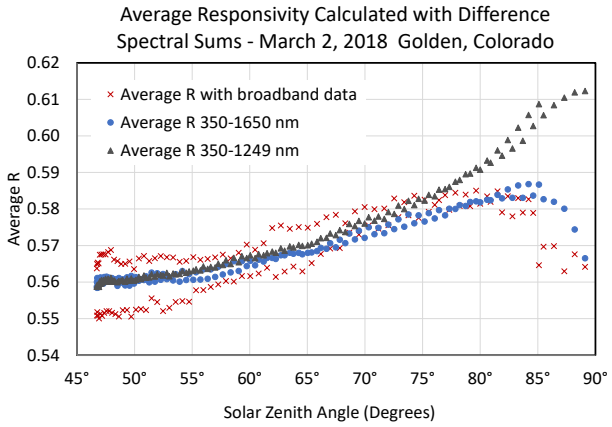

Fig. 3. Comparison of average responsivity calculated with wavelengths from 350 nm to 1249 nm, with wavelengths from 350 nm to 1650 nm and the use of broadband data for the denominator. The three sets of average R values are set equal at 47°.

temperature on the responsivity at a given temperature, and T_{amb} is the ambient temperature. The temperature wavelength dependence is discussed in [3]. The wavelengths are summed from 280 nm to 4000 nm. Measured spectral irradiance data is only available from 350 nm to 1650 nm. The spectral responsivity of the IMT reference cell is small for λ less than 350 nm and is zero for λ 1250 nms and greater. Therefore the numerator can be calculated with the available spectral data. That cannot be said for the denominator that is the sum of irradiance over all wavelengths.

To gauge the importance of the omitting wavelengths from 1650 - 4000 nm in the denominator, the average responsivity is plotted against the solar zenith angle (SZA) in three different ways in Fig. 3: summing over 350 nm to 1249 nm, from 350 nm to 1650 nm, and the broadband pyranometer measurements replacing the sum over all wavelengths in the denominator. Because the IMT responsivity at wavelengths greater than 1250 is zero, the numerator in Eqn. 1 is the same in all three instances. Whereas the denominator will increase by including wavelengths from 1250 nm to 1650 nm or 1250 nm to 4000 nm using broadband data. Because the denominator will be greater the larger the wavelength range, the two shorter interval summations are adjusted to the value obtained using the broadband data at a SZA of 47º. For SZA greater than 70°, the shape of the summations using the 350 nm – 1249 nm start to diverge from the summations using the 350 nm – 1650 nm range. This indicates that the contributions from 1250 nm to 1650 nm are important to consider at larger zenith angles. For SZA values greater than 80º to 85º inclusion of wavelength in the 1650 nm to 4000 nm range seem to affect the comparison. The split in the broadband curve is related to a slight change in the level of the pyranometer. This will be discussed in greater detail in the discussion section of the paper.

At zenith angles less than 70° the three curves are indistinguishable. This implies that the measured wavelength range (350 nm – 1249 nm) adequately describes the complete spectrum and that the wavelength from 1250 nm – 4000 nm are proportional to the wavelength 350 nm to 1249 nm range. It is only at larger SZA that this proportionality breaks down. In the upcoming sections the IMT will be compared to a broadband CMP22 pyranometer. Also the expected output from the IMT will be calculated using the measured spectrum from the spectroradiometer and the spectral response of the instrument. For clarity the spectroradiometers used in this experiment measures from 350 – 1650 nm and the broadband pyranometer is sensitive to the wavelength range 280 – 4000 nm. If the only factor influencing the IMT reference cell was a spectral response, one would expect the calculated IMT values to be similar to the pyranometer values at zenith angles less than 70°. It will be shown that this is not the case.

IV. Comparison with Broadband Data

The postulated relationship between the IMT measurements and broadband measurement is

$$IMT = K \cdot \overline{R}(SZA) \cdot GTI \cdot F(AOI) \qquad (2)$$

where the average responsivity $\overline{R}(SZA)$ is the relative average responsivity determined via Eqn. 1, K represents the constant that translates from relative average responsivity to average responsivity that can be used in analysis, *GTI* is the broadband total irradiance on the one-axis tracking surface, and *F(*AOI) is the angle of incidence function that accounts for the non-linear AOI characteristics of the IMT glazing.

Initially the relationship between the IMT and broadband measurements examined by dividing both sides of Eqn. 2 by *GTI*. A plot the ratio of the IMT reference cell output to the

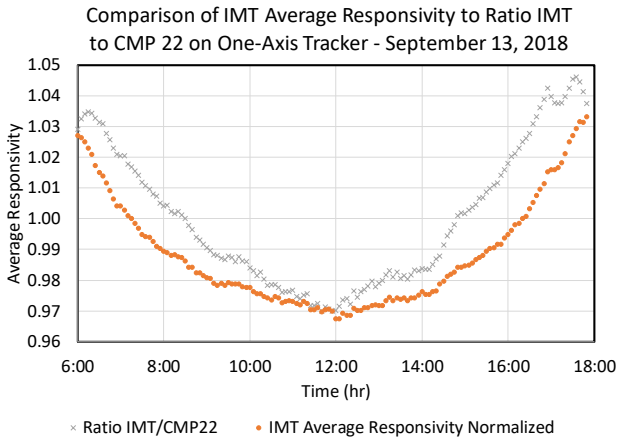

Fig. 4. Ratio of an IMT reference cell to the irradiance measured with a CMP22 pyranometer on a one-axis tracker.

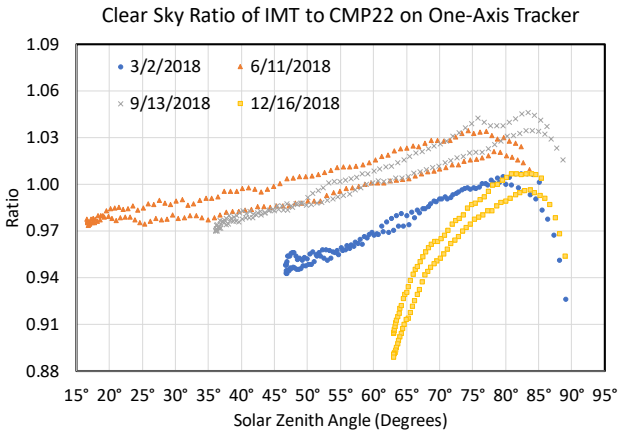

Fig. 5. Ratio of an IMT reference cell to the irradiance measured with a CMP22 pyranometer on a one-axis tracker.

irradiance from a CMP22 pyranometer is shown in Fig. 4 as the grey x's. This was performed under clear skies on September 13, 2018. The ratio varies from about 0.97 at solar noon to about 1.04 in the early morning and late afternoon.

One can also plot the average responsivity determined from Eqn. 1 using the spectral data from 350 nm to 1650 nm. In Fig. 4, this is shown as the brown curve. As with the data in Fig. 3, the average responsivity was normalized to match the ratio of the IMT to GTI measurements at noon.

If the AOI effect was minimal, one would expect the two curves to align. While there is some agreement between the curves, the AOI effects are important to consider and one can begin to gauge the magnitude of the F(AOI) function.

Up to this point, only spectral effects on a clear day were considered. For a more detailed evaluation of the spectral effects at various times of year and to characterize other factors could play a role in the IMT measurements, four days with clear skies at different times of year were selected.

The ratio of the IMT measurements is divided by the GTI measurements (from the CMP22 pyranometer) is plotted against the solar zenith angle in Fig. 5. The IMT values deviates from the CMP22 values. The CMP22 has a small uncertainty, a negligible cosine and temperature response and a uniform wavelength response. The CMP22 is therefor considered the reference that the IMT is trying to mimic. There are 9% or 10% differences over the year. Two main causes are the spectral and AOI effects.

Another way to look at the data is to plot $\overline{R}$ from Eqn. 1 against the AOI for different clear days through the year. The average responsivity of the IMT reference cell is shown in Fig. 6. The same R_λ and T_λ were used for all days and the I_λ and T_{amb} were measured on the specific days examined. The two plots used were generated on the same clear days.

Figure 5 and Figure 6 look significantly different indicating that other features also affect the IMT output or the data from the pyranometer. These are the F(AOI) effects. The value K should be the same for all datasets. Neglected in all analysis is the contribution from spectral irradiance in the 280 nm to 350 nm range. This contribution should be small because the spectral responsivity of the IMT is small at these wavelengths.

The functions in Eqn. 2 can be rearranged to

$$1/(F(AOI)\cdot K) = GTI\cdot \overline{R}\,(SZA)/IMT \qquad (3)$$

Plotting the righthand side of Eqn. 3 isolates the dependence on the F(AOI). This relationship is shown in Fig. 7. The F(AOI) dependence of the reference cells should be very much like the F(AOI) dependence of photovoltaic modules. The data in Fig. 7 are plotted against the angle of incidence. As expected, most of the data falls roughly along the bottom arch.

Fig. 8 is the same as Fig. 7, only using data when the zenith angle is less than 85°. This eliminates many of the extreme points are removed. In Fig. 8, the inverse of a model of F(AOI) function for photovoltaic modules is included in the plot as shown as the black line. There is also a factor K that has to be taken into account. An inverse value of K of 0.633 was used to match the ratio values with the AOI function at 0º AOI.

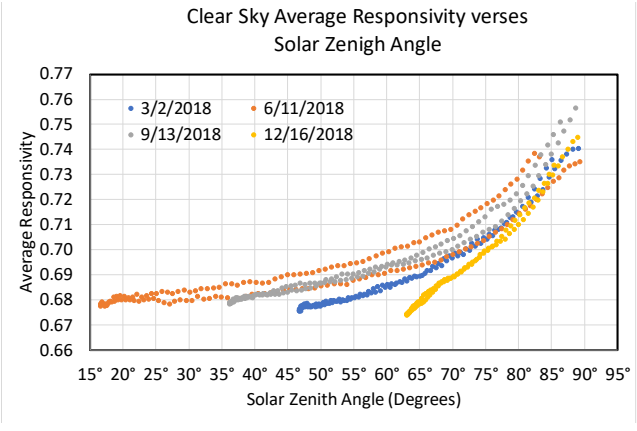

Fig. 6. Plot of IMT reference cell average responsivity plotted against solar zenith angle under clear skies. Reference cell mounted on a one-axis tracker.

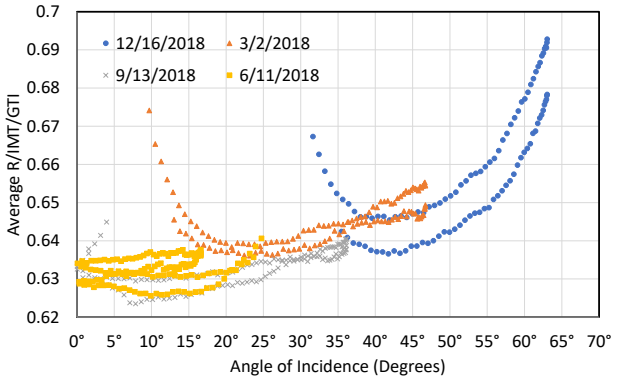

Fig. 7. Ratio of IMT average responsivity divided by the IMT output divided by the measurements of a CMP22 pyranometer on a one-axis tracker plotted against the angle-of-incidence.

Therefore, within 1% to 2%, spectral, temperature, and AOI effects account for most of the difference between the IMT reference cell output and the pyranometer measurements.

V. Comparisons under totally cloudy skies

So far only clear days were examined. The relationships under cloudy skies is more complex because diffuse irradiance becomes the major source of irradiance and the distribution of the diffuse irradiance varies across the sky. In addition, diffuse irradiance under cloudy skies can have a different spectral signature than diffuse irradiance under clear skies and hence affect the references cell differently than under clear skies. Totally cloudy skies were chosen because partially cloudy skies present complex problems with a mixture of both clear sky and cloudy sky spectrum. In addition it is possible to have reflections off the side of clouds on partially cloudy days further complicating the situation.

A plot of average IMT responsivity under totally cloudy skies at four different times during the year are shown in Fig. 9. No

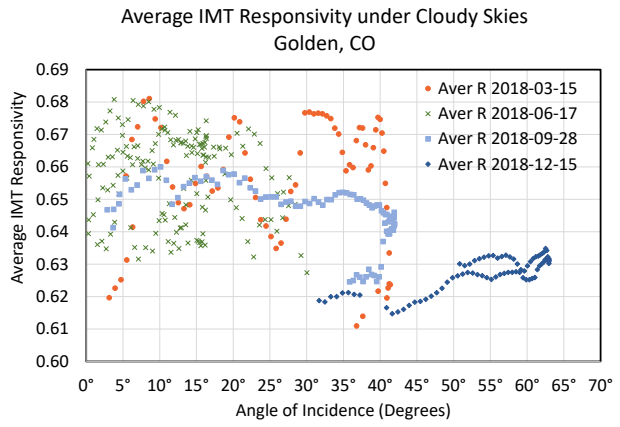

Fig. 9. Average responsivity of an IMT reference cell under totally cloudy skies.

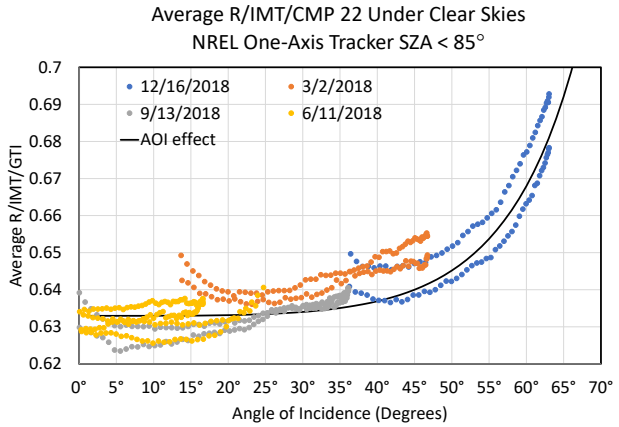

Fig. 8. Same as Fig. 7 with the data limited to SZA < 85°. The AOI effect is plotted and shows that it is important to consider when AOI is greater than 35°.

clear pattern prevails and the overall average IMT responsivity is about 0.65±.03 or about a 5% variation. Applying the ideas from Eqn. 3 to the cloudy data, no visible pattern emerges as shown in Fig. 10.

VI. Discussion of Results

Examination of the IMT reference cells one a one-axis tracker collocated with spectroradiometers covering a 350 nm to 1650 nm range provides a unique opportunity to examine the characteristics of reference cells and pyranometers that are also located on the platform. While it is possible to emulate the pyranometer output to the 2% level under clear skies, it is not practical to use the methodologies show here to model irradiance on a one-axis tracking surface from reference cell data because it is necessary to have coincident spectral data. However, this does tests one's theoretical understanding of the differences between broadband reference pyranometer measurements and reference cell measurements. The results

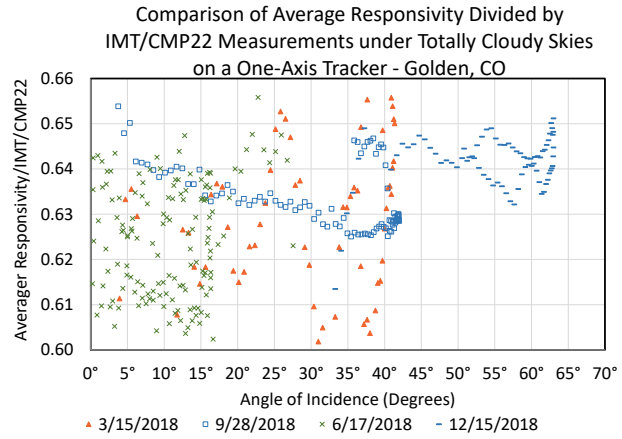

Fig. 10. Average responsivity of an IMT reference cell under totally cloudy skies.

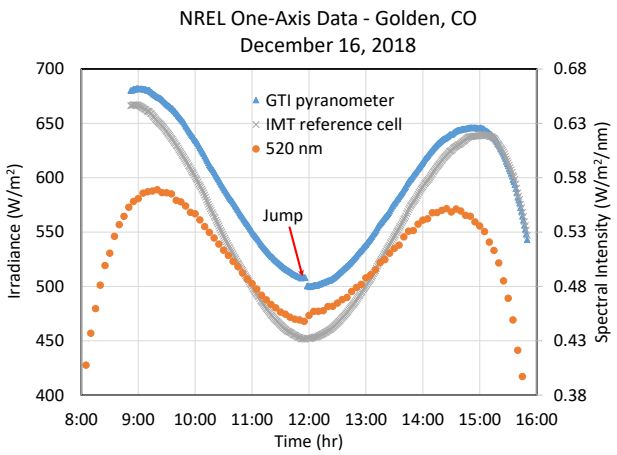

Fig. 11. Measurements from a CMP 22 pyranometer an IMT reference cell and an EKO spectroradiometer on a one-axis tracker. The platform on the EKO tracker rotates 180° at solar noon.

shown here should also be applicable to PV modules because they behave much like reference cells.

As shown in Fig. 5, the difference between the data and the modeled estimate varies over the day. The difference is greatest at large SZA where the path length through the atmosphere significantly affects the spectral distribution. Therefore, one would expect the greatest spectral effects to be in the early morning and late afternoon hours. This is borne out by the modeled results.

There is a slight asymmetry between the morning estimated ratios and the afternoon estimated ratios. One might assign this difference to the influence of temperature on reference cell output. However, the temperature effects have been taken into account. One aspect that has not yet been evaluated is the pyranometer data. As can be seen in Figs. 7 and 8, much of the data seems to have two branches, one for morning data and one for afternoon data.

Fig. 11 illustrates the output of the tilted irradiance from the CMP22, the 520 nm data from an EKO spectroradiometer, and the IMT reference cell on a clear day in December. All three instruments are on an EKO one-axis tracker. The tracker is configured so that the platform upon which the instruments are mounted rotates 180° at solar noon enabling the platform to rotate from east to west during the day. This rotation seems to have little effect on the IMT reference cell, but data from the pyranometer and the spectroradiometer exhibits a 1.5% decrease for December 16, 2018. Other months and other pyranometers also exhibit this effect, although not as much as seen here. The platform is horizontal during this rotation, so north-south alignment of the tracker is not the cause. One possible cause of this change is if platform is tilted 0.2° to the south. Then when it is rotated 180° it would be tilted 0.2° to the north. If one assumes that the global irradiance is mostly dependent upon the direct normal irradiance times the cosine of the solar zenith, this change as seen in the middle of December would be 1.5%. The spectroradiometer is on the opposite side of the platform than the pyranometer and sees the opposite effect. Since the pyranometer acts as a reference measurement and the spectral data are used to determine the average responsivity of the IMT reference cell, this problem should be considered before any firm conclusion is drawn from the results. This is also a good example for checking all the measurements along with the measurements of the test subject.

As mentioned earlier, the uncertainty with the broadband pyranometer measurements is on the order of ±3.5%. Of course, the relative uncertainty can be much less. The cosine response of the pyranometer is good, but deviations from a true cosine response are incorporated into the quoted uncertainty.

Not covered in this discussion is the uncertainties in the IMT measurements. The IMT calibration value was determined in the lab and not in the field. If it was determined in the field, the value would be dependent upon the spectral distribution of the incident radiation at the time of calibration.

This is related to the effects of temperature and higher temperatures in the afternoon should increase the responsivity. However, this doesn't significantly change the general shape of the modeled effect.

The other factor that could influence the shape of the ratio is the angle of incident effects. For the one-axis tracker in mid-September, the angle of incident changes from about 30º at noon to 0º just after sunrise and just after sunset. A simple model of the angle of incidence affect [5] is illustrated in Fig. 8. This model is based on the physics of transmission of light through glass and is very rigorous at small angles of incidence. At larger angles, spectral effects make it difficult to test the model. This angle of incidence model is for both direct normal and diffuse irradiance incident on the surface.

If the spectral, temperature, and angle of incident effects are ruled out, that only leaves the cosine response characteristics of the Class A pyranometer or the spectroradiometer as a source of difference between the model and the data. This is a one percent difference, so it is not outside the realm of possibilities and cannot be ruled out. So even with the best instrumentation there is a limit to how well one can test a model.

The comparisons so far require that the denominator in Eqn. 1 give a fair representation of the broadband spectrum over the day. One can substitute the broadband measurements for this sum over wavelength in Eqn. 1 and this GTI value would cancel out in Eqn. 3 leaving

$$F(AOI)\cdot K = \frac{IMT}{\sum_{280nm}^{4000nm} R_\lambda[1+T_\lambda(T_{amb}-25)]\cdot I_\lambda} \qquad (4)$$

where the denominator is the numerator in Eqn. 1. Given spectral measurements with little or known biases, a good measurement of F(AOI) could be obtained to test against F(AOI) models.

Using Eqn. 4, one can check the modeling assumption by calculating the IMT output against the measured IMT values. *F(AOI)*, R_λ, and T_λ values are fixed and I_λ is measured. Only the

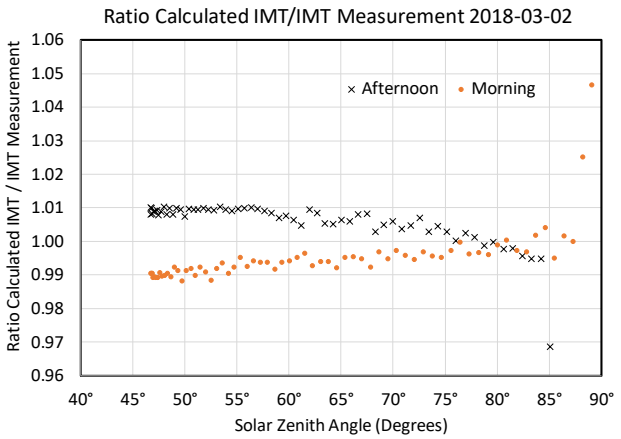

Fig. 12. Comparison of the modeled verse the modeled IMT values on a clear day - March 3, 2018. The morning values are circles and the afternoon values are x's. In this example, the noonday values have the smallest solar zenith angles while having the largest angles-of-incidence.

constant K is scalable. This allows a direct comparison between the IMT measurements and the spectral measurements. Instead of plotting the calculated IMT values against measured IMT values, the ratio is plotted in Fig. 12. A value of 1.72 was used for *K* in the example shown. The change seen at 47° is the result of a slight tilt of the spectroradiometer to the north in the morning. As has been discussed, as the tracker platform rotates 180° at solar noon, the spectroradiometer is tilted slightly to the south in the afternoon. This results in the split in the data shown in Fig. 12. Given the uncertainties in the measurements and the assumptions made, this comparison provides confidence in the methodology used.

VII. Next Steps

Before speculating on possible causes of the difference between modeled and measure results, more data should be examined in detail and against a variety of environmental parameters. A similar experiment is underway in Eugene, Oregon with a spectroradiometer that measured irradiance from 350 nm to 1050 nm. To compare the results with those obtained in Golden, Colorado, the spectral distribution at 1050 to 1249 nm has to be modeled. In addition, the spectral distribution between 280 nm and 350 nm should also be modeled. Modeling irradiance, let alone spectral irradiance on a tilted or one-axis tracking surface has large uncertainties. When calculating the average responsivity on a horizontal where the full 280 nm to 4000 nm spectral distribution can be modeled, one should be able to identify the effects of limiting the spectral range to 350 nm to 1650 nm or even just to 350 nm to 1050 nm. For horizontal evaluations, a precise model of the angle-of-incident effects is needed.

To minimize the angle-of-incidents effects and just concentrate on the spectral and temperature effects, an experiment should be performed on a two-axis tracker. Angle of incidents effects will always be present because the diffuse and ground reflected irradiance also contribute to the total irradiance on a tilted surface. However, the direct normal irradiance, which is the major contributor to the irradiance on an instrument mounted on a two-axis tracking surface. The diffuse and ground reflect irradiance should be minimal under clear skies with no snow on the ground.

VIII. Significance of Findings

Reference cells are used to make a number of field tests. If these tests are ever to be generalized and compared to tests using other instruments at different tilts and orientations, the systematic biases of reference cells need to be clearly understood. The preliminary finding of this study shows that changes in spectral irradiance are a big source of bias, but angle-of-incidence effects are also important. While temperature effects were included in this study, they are much smaller than the spectral and angle of incidence effects. Tracking down these other sources will provide the basis for more accurate modeling and testing.

When modeling the effects of changes in the spectral distribution over the day, the need to use information on the spectral characteristics in the 1250 nm to 1650 nm range were found to be important at large zenith angles. It is expected that the spectral distribution in the 1650 nm to 4000 nm play a role, especially at very large solar zenith angles. It will be difficult to model the spectral irradiance on tilted or one-axis tracking surfaces with a sufficient accuracy to compare broadband measurements with measurements from reference cells even though reference cells typically are insensitive to irradiance greater than 1250 nm. Broadband instruments are sensitive to all wavelengths.

Acknowledgments

This work was supported by Alliance for Sustainable Energy, LLC, the manager and operator of the National Renewable Energy Laboratory for the U.S. Department of Energy (DOE) under Contract No. DE-AC36-08GO28308. Funding provided by the U.S. Department of Energy Office of Energy Efficiency and Renewable Energy Solar Energy Technologies Office. The views expressed in the article do not necessarily represent the views of the DOE or the U.S. Government. The U.S. Government retains and the publisher, by accepting the article for publication, acknowledges that the U.S. Government retains a nonexclusive, paid-up, irrevocable, worldwide license to publish or reproduce the published form of this work, or allow others to do so, for U.S. Government purposes. We also thank the other sponsors of the UO Solar Radiation Monitoring

Laboratory, the Bonneville Power Administration, the Energy Trust of Oregon and Portland General Electric.

REFERENCES

[1] Vignola, F., Chun-Yu Chiu, Josh Peterson, Michael Dooraghi, Manajit Sengupta, Comparison and Analysis of Instruments Measuring Plane-of-Array Irradiance for One-Axis Tracking PV Systems, IEEE-PVSC -44, 2017.

[2] Vignola, F., Josh Peterson, Chun-Yu Chiu, Michael Dooraghi, Manajit Sengupta, Fotis Mavromatakis, Comparison of Pyranometers and Reference Cells on Fixed and One-Axis Tracking Surfaces, American Solar Energy Society Solar Conference, 2017.

[3] Vignola, F., Chun-Yu Chiu, Josh Peterson, Michael Dooraghi, Manajit Sengupta, Evaluation of Photodiode-based Pyranometers and Reference Solar Cells on a Two-Axis Tracking System, IEEE-PVSC – 45, 2018.

[4] Hishikawa, Yoshihiro, Masahiro Yoshita, Hironori Ohshima, Kengo Yamagoe, Haruya Shimura, Ayumi Sasaki, and Takashi Ueda, 2018. Temperature dependence of the short circuit current and spectral responsivity of various kinds of crystalline silicon photovoltaic devices, Japanese Journal of Applied Physics 57, 08RG17 (2018)

[5] Marion, B. “Numerical method for angle-of-incidence correction factors for diffuse radiation incident photovoltaic modules”, Sol. Energy Solar Energy 147 (2017) 344–348